European Journal of Medicinal Chemistry 44 (2009) 4485–4489

Contents lists available at ScienceDirect

European Journal of Medicinal Chemistry

journal homepage: http://www.elsevier.com/locate/ejmech

Original article

3D QSAR study of the toxicity of trichothecene mycotoxins

Wayne E. Steinmetz [a,*], Cezar B. Rodarte [b], Alvin Lin [a]

[a] Chemistry Department, Pomona College, Claremont, CA 91711, USA
[b] Chemistry Department, University of Redlands, Redlands, CA 92373, USA

ARTICLE INFO

Article history:
Received 22 April 2009
Received in revised form
22 May 2009
Accepted 10 June 2009
Available online 18 June 2009

Keywords:
Trichothecene mycotoxins
3D QSAR
CoMFA
CoMSIA

ABSTRACT

Trichothecene mycotoxins, toxic natural products of fungi from the family *Hypocreaceae*, are potent inhibitors of protein synthesis. The application of 3D QSAR to these toxins explored the structural basis for their biological activities. A CoMFA ($Q^2 = 0.619$, $R^2 = 0.921$) model was developed for a set of 15 toxins with the trichothecene nucleus; CoMFA ($Q^2 = 0.518$, $R^2 = 0.855$) and CoMSIA ($Q^2 = 0.695$, $R^2 = 0.960$) models were developed for 31 toxins with the nucleus and a macrolide ring. The results show the role of electrostatics and steric factors in the activity of the toxins and indicate that the conformation of the macrolide ring influences the toxicity of the macrolide toxins.

1. Introduction

Species of fungi from the genera *Fusaria*, *Trichoderma*, and *Myrothecium* in the family *Hypocreaceae* produce highly toxic trichothecene mycotoxins which inhibit protein synthesis and induce apoptosis [1,2]. These fungi pose significant public health problems because they infect grain products such as corn and barley [3]. In the Midwest, where cattle are fed corn, the toxins from contaminated grain present a greater risk to the health of farm animals than aflotoxins [4]. Trichothecene mycotoxins have also been claimed as components of yellow rain, a chemical agent used by the Soviet army in Afghanistan and Southeast Asia [1,5].

All trichothecene mycotoxins contain a characteristic trichothecene nucleus, a rigid tetracyclic ring system (Fig. 1). The 12,13-epoxide group is the functionality responsible for the biological activity of the toxins and its removal leads to complete loss of toxicity [6,7]. The toxicity of known mycotoxins spans orders of magnitude and is modulated by substitution of the trichothecene core. Particularly potent are the macrolide mycotoxins in which the groups R and R′ attached to carbons 4 and 6, respectively, constitute a macrolide ring. Verrucarin A and roridin A (Fig. 2) are representative macrolide mycotoxins.

QSAR, the quantitative study of the dependence of biological activity on chemical structure, is a powerful method that has been routinely employed in the design of new drugs and the understanding of toxicity [8]. Although several groups have examined of structure–activity relationships of mycotoxins [9], there are no published QSAR studies of this class of toxins. Our application of NMR spectroscopy and molecular modeling to the conformation and dynamics of two macrolide mycotoxins, roridin A and verrucarin A, raised the question of the dependence of toxicity on molecular conformation [10]. Our preliminary 2D QSAR calculations indicated that answering this question would require the analysis of a large data set with 3D QSAR methodology. We report the successful application of CoMFA, a 3D QSAR method, to a set of 32 macrolide mycotoxins and also to a set of 15 toxins with only the trichothecene nucleus. Our models can be used to predict quantitatively the properties of trichothecene toxins not in the data set, but the primary objective of this study is an examination of the structural basis for their biological activity. The results provide insights into the effect of substitution and show that conformation does to some extent affect activity.

CoMFA, comparative molecular field analysis, is a 3D QSAR method well suited for exploring the dependence of activity on conformation. The method established by Cramer et al. consists of five steps [11]. (1) Obtain the 3D structures of the compounds, either from crystallography or molecular modeling. Crystal structures are only available for small number of mycotoxins. We employed molecular mechanics with the Merck Molecular Force Field (MMFF94) as our work with roridin A and verrucarin A

* Corresponding author. Tel.: +1 909 621 8447; fax: +1 909 607 7726.
E-mail addresses: wsteinmetz@pomona.edu (W.E. Steinmetz), cezar_rodarte@redlands.edu (C.B. Rodarte), al002005@pomona.edu (A. Lin).

0223-5234/$ – see front matter © 2009 Elsevier Masson SAS. All rights reserved.
doi:10.1016/j.ejmech.2009.06.012

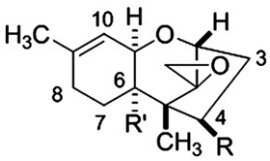

Fig. 1. Covalent structure of the trichothecene nucleus.

showed that modeling yielded results in excellent agreement with the NMR data [10]. Many biomolecules such as the macrolide mycotoxins are flexible and the set of structures includes the global energy minima and conformations close in energy to the minimum. (2) Superimpose the structures using conserved features of the molecule, the heavy atoms in the trichothecene nucleus in our case. (3) Embed the set of superimposed structures in a three-dimensional grid. For each structure calculate the electrostatic energy with a test charge (C^+) at each grid point outside the van der Waals surface. The set of energies at the grid points defines the electrostatic CoMFA field. A corresponding steric CoMFA field is defined by the Lennard–Jones potential energy with a test atom (sp^3C) at the grid points. Other fields such as CoMSIA can also be defined [12,13]. (4) Correlate a quantitative measure of biological activity such as $\log_{10}(LD_{50})$ with the probe interaction energies that define the CoMFA fields. Conventional regression analysis, the approach in classical 2D QSAR, cannot be used as the number of grid points far exceeds the number of dependent variables. Instead one employs partial least squares (PLS) where the changes in biological activity are correlated with linear combinations of changes in the interaction energies. (5) Analyze the results to identify the energetic origins of changes in activity associated with variation in molecular structure. In 2D QSAR the model is represented by a regression equation. In contrast, CoMFA yields color-coded contour maps which identify regions where changes in the fields are associated with an increase or decrease in the biological activity. The final model is geometric rather than algebraic in nature since the underlying basis of CoMFA is 3D molecular structure.

The literature yielded two data sets suitable for a CoMFA analysis. All compounds in the data set must have a well defined covalent structure and stereochemistry [14]. Considerable effort was required to satisfy these conditions and compounds were not included in the analysis if the literature lacked a clear assignment of their stereochemistry. An ideal data set should be large enough to provide 4–5 compounds per PLS component and enable a separation into a learning (L) set and a test (T) set. Jarvis et al. measured the ability of macrolide mycotoxins to extend the life span of mice inoculated with P-388 mouse leukemia and their data presumably reflect the effect of the toxins on the leukemia cells [15,16]. Their quantitative measure of activity is *R*, 100 times the ratio of the days test animals lived over the days control animals lived. The effect of substitution on the trichothecene nucleus is provided by the work of Madhyastha et al. who reported the relative toxicity to yeast cells of a set of 15 toxins (RX) [17]. Tables 1 and 2 provide a list of the compounds in the data sets and values of *R* and RX. The Supplementary data provide values of the 2D QSAR parameters NVE and clogP as well as the structure and stereochemistry of each compound.

2. Methods

Values of the octanol/water partition coefficient for each mycotoxin were calculated with the ClogP module of Bio-Loom (BioByte, Claremont, CA). Hartree-Fock calculations with 3-21G basis functions and preliminary modeling steps were conducted using Version '06 of Spartan (Wavefunction, Irvine, CA). Versions 7.3 and 8.0 of SYBYL (Tripos, Inc., St. Louis, MO) were used for all phases of the CoMFA analysis. Default parameters were used with the following changes in Random Search parameters: Bump Factors, 0.02; Ring Bond closure, 10 Å; energy cutoff, 418 kJ/mol.

The molecular structure of each mycotoxin was drawn via the Sketch module in SYBYL. The NMR structure of roridin A or verrucarin A was used as a root structure in this step [10]. After verification of the stereochemistry, energy minimization with a conjugate-gradient minimizer and the MMFF94 force field was followed by 10 000 or more cycles of the Random Search algorithm. As shown in our work on derivatives of erythromycin [18], this strategy identified the global minimum and structures within 8 kJ/mol of the global minimum. Using the heavy atoms in the trichothecene nucleus, oxygen 1 and carbons 2 through 12, the Fit module was employed to superimpose all structures. Two sets of structures were assembled, one consisting of mycotoxins with a macrolide ring (MAC) and a second consisting of those without (TRI). The members of each set were embedded in a rectangular grid with a spacing of 2 Å and 2016 and 1200 grid points for the MAC and TRI sets, respectively. The MMFF94 yielded the partial charges required for the calculation of the CoMFA electrostatic field. The generation of the CoMFA and COMSIA fields employed the default probe, a sp^3 hybridized C^+ test charge with a H-bond donor, an acceptor property of +1, a hydrophobicity of +1, a cutoff energy of 30 kcal/mol (126 kJ/mol), and an attenuation factor α of 30. For each physicochemical property such as H-bond donating ability, the CoMSIA field at each grid point, designated as a similarity index, is a weighted sum over the atoms in the molecule. Each term in the sum is the product of a property of the atom with that of the probe atom.

The PLS analysis used the base 10 logarithm of the biological activity as the dependent variable. The full data set was used in the development of the 3D QSAR model. The data were then divided into a learning (L) set which was used to derive the final model and a small test (T) set which was used to validate the final model. Compounds chosen from the full data set for the T set contained functionality represented by several compounds in the full data set. For example, 8-oxoverrucarin A is not a candidate for the T set as it is the only toxin in the MAC data set with a carbonyl substituent at the 8 position. In contrast, α-9,10-expoxy verrucarin A was included in the T set as the 9,10-epoxy substitution and the verrucarin family of macrolide toxins are well represented in the full data set. As noted by Eriksson et al. [19], the final characteristics including the

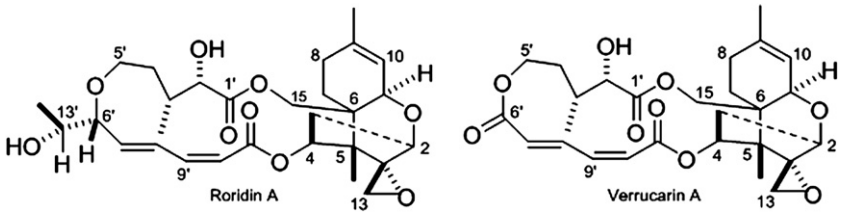

Fig. 2. Structure of two macrolide trichothecene mycotoxins.

Table 1
Experimental and predicted activity of macrolide trichothecene mycotoxins (MAC data set).

Compound	L/T[a]	R[b]	$\log_{10} R$		
		exp.	exp.	pred.	
				CoMFA[c]	CoMSIA[d]
1. Verrucarin A	L	127	2.104	2.083	2.104
2. Verrucarin B	L	142	2.152	2.107	2.117
3. Verrucarin J	L	150	2.176	2.136	2.127
4. Roridin A	L	128	2.107	2.146	2.129
5. Roridin D	L	131	2.117	2.120	2.112
6. Roridin H	L	158	2.199	2.061	2.102
7. Baccharin B1	T	214	2.330	2.319	2.414
8. Baccharin B2	L	278	2.440	2.422	2.417
9. Baccharin B3	L	250	2.398	2.323	2.340
10. Baccharin B4	T	185	2.267	2.307	2.249
11. Baccharin B5	O	311	2.493	2.231	2.252
12. Baccharin B6	L	166	2.220	2.254	2.202
13. Baccharin B7	L	196	2.292	2.323	2.340
14. Baccharin B8	L	233	2.367	2.330	2.362
15. β-9,10-Epoxy verrucarin A	L	210	2.322	2.318	2.323
16. β-9,10-Epoxy verrucarin A acetate	L	172	2.236	2.246	2.283
17. α-9,10-Epoxy verrucarin A	T	118	2.072	2.026	2.100
18. β-8-Hydroxy verrucarin A	L	132	2.121	2.219	2.213
19. 8-Oxoverrucarin A	L	122	2.086	2.177	2.093
20. 16-Hydroxy verrucarin A	L	190	2.279	2.257	2.282
21. β-9-Hydroxy, α-bromo verrucarin A	L	133	2.124	2.076	2.107
22. β-9,10-Epoxy verrucarin B	L	157	2.196	2.206	2.240
23. β-9,10-Epoxy roridin A	L	205	2.312	2.301	2.310
24. β-8-Hydroxy roridin A	L	156	2.193	2.282	2.329
25. β-Hydroxy verrucarin J	L	181	2.258	2.291	2.217
26. β-9,10-Epoxy roridin H	L	172	2.236	2.276	2.265
27. β-9,10-Epoxy verrucarin J	T	172	2.236	2.195	2.253
28. 16-Hydroxy roridin A	L	258	2.412	2.408	2.403
29. β-8-Hydroxy, β-9,10-epoxy verrucarin A	L	321	2.507	2.426	2.421
30. β-8-Hydroxy, β-9,10-epoxy roridin A	L	321	2.507	2.548	2.488
31. 16-Hydroxy, β-9,10-epoxy verrucarin A	T	203	2.307	2.153	2.362
32. 16-Hydroxy, β-9,10-epoxy roridin A	L	321	2.507	2.452	2.553

[a] T/L: T, member of the T set; L = member of the L set; O, outlier in PLS analysis of $\log_{10} R$.
[b] R: measure of extension of life span of mice inoculated with leukemia cells,100 × (life span after inoculation with exposure to a mycotoxin)/(life span after inoculation of control animals); data from Ref. [11,12].
[c] pred.: value predicted from the CoMFA and CoMFIA models based on the L set.
[d] pred.: value predicted from the CoMFA and CoMFIA models based on the L set.

selection of descriptors should be based entirely on the L set with no contribution from the T set. The development of the 3D QSAR model was guided by the leave-one-out cross-validated PLS parameters: s_{CV}, the cross-validated standard deviation, and Q^2, the cross-validated value of R^2. The use of only conformers at the global minimum yielded an unsatisfactory model, one with a large s_{CV} and $Q^2 < 0.3$, irrespective of the choice of fields. However, an examination of the predicted value of the dependent variable, e.g. $\log_{10} R$, for each conformer of each toxin identified after several PLS cycles a set of conformers whose fields correlated well with the biological activity. The examination of the table of predicted values identified a single outlier in the two data sets, baccharin B5 in the MAC data set. Its exclusion led to a significant improvement in the PLS statistics. We are unable to provide a satisfying explanation for its poor fit. The optimal model was identified by the minimum value of s_{CV} which also corresponded with the maximum Q^2. The dependence of the leave-one-out statistics on the number of components is provided in the Supplementary data. We deliberately focused on s_{CV} rather than Q^2 in order to avoid overfitting. The SYBYL PLS routine bases the number of components on the maximum of Q^2 and when employed uncritically leads to models with an excessive number of components. Once the cross-validated statistics identified the number of PLS components, the optimum set of conformers, and the CoMFA fields, a non-cross-validated PLS run on the L set generated the final model which was used to predict the properties of the compounds in the T set. The two standard deviations – s_L, the non-cross-validated s using the L set, and s_T, s calculated from the T set – were compared using the F test. The results of these calculations yielded statistically significant results and are summarized in Table 3. The Supplementary data provide additional PLS statistic including statistics for rejected models.

Table 2
Experimental and predicted activity of trichothecene mycotoxins (TRI dataset).

Compound	T/L[a]	RX[b]	$\log_{10}$ RX	
		exp.	exp.	pred.[c]
1. Acetyl T2 toxin (AT-2)	L	17.6	1.245	1.470
2. Diacetoxyscirpenol (DAS)	L	342.9	2.535	2.516
3. Deoxynivalenol (DON)	L	5.7	0.756	0.437
4. Fusarenon-X (FUSX)	L	6.4	0.806	1.144
5. HT-2 toxin	T	66.7	1.824	2.153
6. Monoacetoxyscirpenol (MAS)	L	42.1	1.624	1.595
7. Nivalenol (NIV)	T	1.3	0.114	0.398
8. Neosolaniol (NSL)	L	4.4	0.644	0.650
9. 4-Hydroxy T2 toxin (T2-4ol)	L	4.3	0.63	0.514
10. T2 toxin	L	2400	3.380	2.968
11. 15-Acetyl deoxynivalenol (ADON)	L	13.3	1.124	1.392
12. Acetyl diacetoxyscirpenol (ADAS)	T	2.2	0.342	−0.109
13. Iso-T2 toxin	L	1.9	0.279	0.611
14. Triol of T2 toxin (T2-3ol)	L	8.7	0.940	1.030
15. Tetraol, tetracetate of T2 toxin (T2-4A)	L	1	0.000	−0.361

[a] T/L: T, member of the T set; L = member of the L set.
[b] RX: toxicity of yeast cells to mycotoxins relative to T2-4A; data from Ref. [13].
[c] pred.: value predicted from the best CoMFA model based on the L set.

3. Discussion of the results

3.1. Macrolide mycotoxins (MAC data set)

The MAC data set of 31 toxins, divided into an L set of 26 compounds and a T set of 5, yielded a credible 3D QSAR model even though the values of $\log_{10} R$ span less than half a log unit. All relevant parameters including the standard deviation for the T set, s(T), pass the F test at the 95% confidence level for statistical significance. Normally, the dependent variable in a successful QSAR analysis spans at least three log units. Given the limited range in $\log_{10} R$ and molecular formula, it is not surprising that $\log_{10} R$ does not correlate with 2D QSAR parameters. The development of statistically significant CoMFA and CoMSIA models for the MAC data set is remarkable and shows the power of 3D QSAR to handle subtle trends. The successful fit also hinges on the quality of the data. The regression statistics for the correlation of $\log_{10} R$ with the number of valence electrons (NVE) were $Q^2 = 0.192$, $R^2 = 0.092$ and with log P were $Q^2 = 0.193$, $R^2 = 0.293$. In contrast, the CoMFA fit on the same compounds yielded $Q^2 = 0.518$ and $R^2 = 0.855$. The vast improvement demonstrates the value of 3D QSAR. The CoMFA fields yielded an acceptable model in which steric and electrostatic

Table 3
PLS statistics for the development of the CoMFA/COMSIA models.

Dep. var.	N_L	N_T	Field	c	s_{cv}	Q^2	s(L)	R^2	s(T)	F_r	f(S,D)	f(E,A)
log R	26	5	CoMFA	3	0.103	0.498	0.053	0.868	0.077	0.79	0.37	0.63
log R	31	0	CoMFA	3	0.095	0.518	0.052	0.855			0.37	0.63
log R	26	5	CoMSIA	5	0.092	0.633	0.044	0.916	0.047	0.42	0.40	0.60
log R	31	0	CoMSIA	5	0.079	0.695	0.044	0.960			0.40	0.60
log RX	12	3	CoMFA	3	0.88	0.379	0.31	0.923	0.38	0.39	1.00	0.00
log RX	15	0	CoMFA	3	0.65	0.619	0.30	0.921			1.00	0.00

N_L and N_T, number of compounds in the L and T sets, respectively.
f(X), fractional contribution of the field to the PLS components; X = S and E for steric and electrostatic CoMFA fields X = D and A for donor and acceptor CoMSIA fields.
$F_r = [s(T)^2/s(L)^2]/F(N_T, N_L - c)$. A value less than one supports the null hypothesis and validates the model.

factors make important contributions to the activity but electrostatics is more important. Even better statistics were obtained with a H-bond donor/acceptor CoMSIA field. The PLS statistics for the final model are summarized in Table 3.

Fig. 3 shows the 3D contours maps for the CoMFA and CoMSIA models. For the most part, the surfaces which identify factors which increase or decrease $\log_{10} R$ span regions of substitution in the set of macrolide toxins. The CoMSIA contour map shows the importance of hydrogen bonding in the binding of mycotoxins to the ribosome. Particularly prominent are the regions around carbons 9–10 and carbon 6′. The latter reflects the differences in activity between the roridin and verrucarin families of toxins and the CoMFA contour map indicates that the differences are due to a combination of steric and electrostatic factors. Carbons 7′ and 8′ are unsubstituted in the MAC data set. The CoMFA and COMSIA contours flanking them show that conformation of the macrolide ring plays a role in the variation of activity with molecular structure.

The CoMFA results inform the role of the 9, 10 center in activity. Jarvis et al. concluded that epoxidation at carbons 9 and 10 would lead to an increase in activity [15,16]. The CoMFA contour map shows that this effect is electrostatic in nature. The blue surface means that a decrease in the electrostatic energy with the positive test probe, a consequence of a lower electrostatic potential on the surface and more negative partial charges on the atoms, results in an increase in $\log_{10} R$. Qualitatively, epoxidation, the insertion of highly electronegative oxygen into the double bond, has exactly this effect. Furthermore, reduction of the double bond will modify the Coulombic environment in the opposite direction and lead to a reduction in $\log_{10} R$. The CoMFA results clarify an observation by Wei and McLaughlin that hydrogenation of the 9,10 double bond leads to a strong reduction in activity [20]. These observations are supported by a set of test calculations of the electrostatic potential at the van der Waals surface from the Hartree-Fock wave function. The electrostatic energy with a positive test charge yields the series $C_2H_6 > C_2H_4 > C_2H_4O$, in parallel with the trend in activity.

3.2. Toxins with only the trichothecene nucleus (TRI data set)

Although values of $\log_{10}$ RX span more than 3 log units, the TRI data set of 15 toxins did not yield a correlation with log *P* and NVE. The statistics for the regressions are log *P*: $R^2 = 0.033$, $Q^2 = -0.304$ and NVE: $R^2 = 0.169$, $Q^2 = -0.115$. As in the case of the MAC data set, it does yield an excellent CoMFA model. The final model, with a T set of 12 compounds and an L set of 3, has only a steric field and is well validated by the PLS statistics and the T set. In this case, there are no outliers and models based on CoMSIA fields yielded poorer rather than improved statistics. The compounds in the T set had to be chosen carefully as the smaller TRI data set had less redundancy than the MAC data set; a random selection from the full data set yielded a model with a negative Q^2. The statistics would probably dramatically improve with a larger data set that better samples chemical space. The contour map (Fig. 4) shows the steric influence of substituents on carbons 3, 4, and 6. The green contour by carbons 4 and 6 suggests a fit of their substituents to a cleft in the binding site which leads to an attractive van der Waals interaction and enhanced activity. The yellow contour by carbon 3 indicates the reverse. Presumably larger substituents interact repulsively with the binding site and lead to reduced activity.

3.3. Relation of the CoMFA results to structures of the ribosome

It is well known that trichothecene mycotoxins inhibit protein synthesis by binding to peptidyltransferase at the 60S ribosomal subunit [21]. The toxins examined here act by blocking the

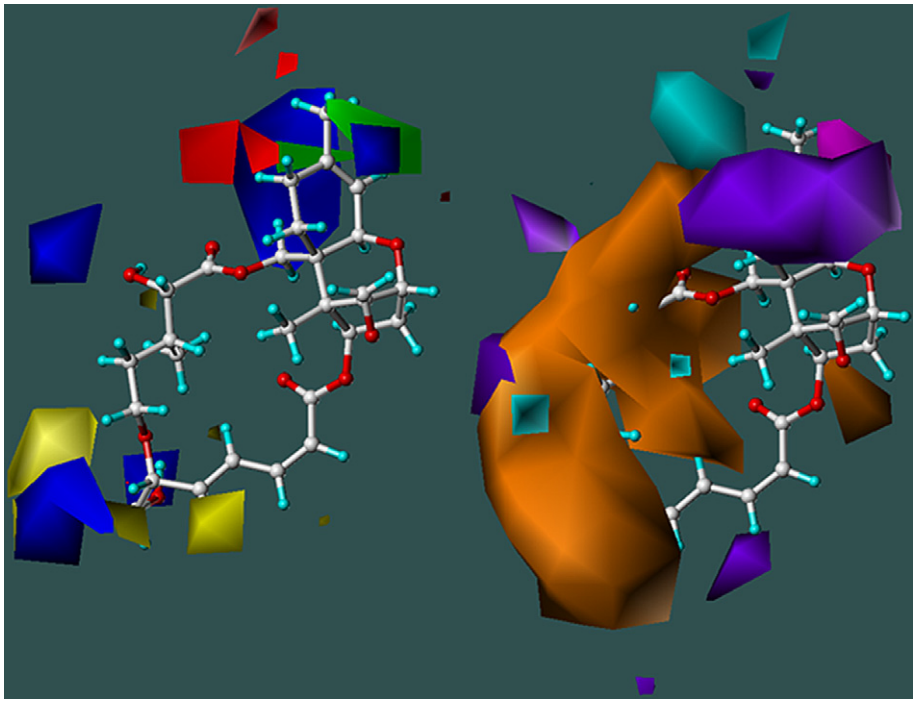

Fig. 3. 3D contour maps (standard deviation × coefficient) for the MAC data set. The molecule is roridin A. Left: CoMFA contour map. Within the volume identified by the green (yellow) surface, changes in the toxin yielding an increase in the Lennard–Jones steric energy with the sp^3 C^+ test probe lead to an increase (decrease) in the dependent variable. The red (blue) surfaces identify where structural changes yielding a decrease in the electrostatic (Coulombic) energy with the probe lead to a decrease (increase) in the dependent variable. Right: CoMSIA contour map. In the region identified by cyan (purple) contours, an increase in the H-donor field leads to an increase (decrease) in $\log_{10} R$. Similarly, the magenta (orange) contours identify regions where an increase in the H-acceptor field is tied to an increase (decrease) in activity. (For interpretation of the references to color in this figure legend, the reader is referred to the web version of this article.)

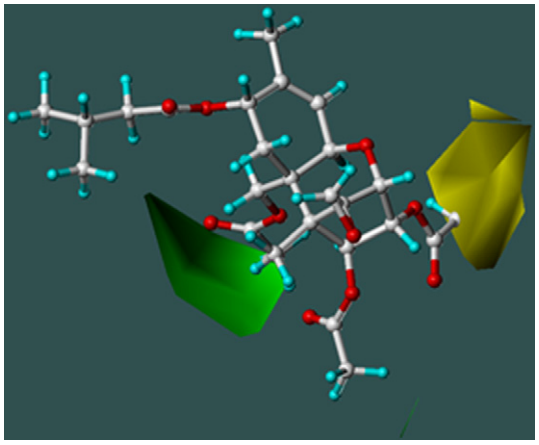

Fig. 4. CoMFA contour map (standard deviation × coefficient) for the TRI data set. The model employs only a steric field. The molecule is T-2 toxin. The color scheme is defined in the caption to Fig. 1.

initiation step at the ribosome [22]. Furthermore, toxins such as T-2 toxin are factors in the promotion of apoptosis [2]. Although no crystal structures of ribosomal bound trichothecene mycotoxins have been published, Li and Petska have shown DON and T-2 toxin induce cleavage at A6390 and A4045 in the peptidyltransferase center of yeast 28S ribosomal RNA [23]. The site of cleavage is close to the binding sites determined crystallographically for the antibiotics anisomycin, chloramphenicol, sparsomycin, blasticidin S, and virginiamycin M [24]. Each antibiotic binds at a separate site which is in close to the peptidyltransferase center. The proximity of their binding sites to the peptidyltransferase center indicates elements of selectivity but the range of binding sites suggests that several factors are responsible for binding and chemical activity. The importance of the steric factors in the CoMFA results is consistent with their location in a pocket away from the surface. In the absence of a crystal structure, we cannot determine the exact locus of the electrostatic interactions involving carbons 9 and 10 in the macrolide toxins. The macrolide ring of the macrolide mycotoxins might bind in the binding site for virginiamycin M, itself a macrolide with a comparable size.

4. Conclusion

This study shows the value of 3D QSAR in general and CoMFA and CoMSIA in particular for the task of exploring the structural origins of the trends in mycotoxins activity. Validation with the T sets indicates that the models also have predictive value. 3D QSAR yielded a statistically valid models in two cases where 2D QSAR failed. The CoMFA and CoMSIA models for the MAC data set provided complimentary pictures for the activity of macrolide mycotoxins. Both models provide evidence of a direct influence of conformation on activity. The model will have further utility in the interpretation of the crystal structure of ribosomally bound mycotoxins once they are available.

Acknowledgments

We dedicate this paper to Corwin H. Hansch, the developer of QSAR and a supporting colleague. Two of us, AL and CBR, are indebted to Pomona College and the University of Redlands for undergraduate summer research fellowships. We also acknowledge BioByte for a donation of the Bio-Loom software.

Appendix. Supplementary data

Supplementary data associated with this article can be found in the online version at doi:10.1016/j.ejmech.2009.06.012.

References

[1] W. Augerson, A Review of the Scientific Literature as it Pertains to Gulf War Illnesses, vol. 5, Rand Corp., Santa Monica, CA, 2000, (Chapter 4).
[2] K. Doi, N. Ishigami, S. Sehata, Int. J. Mol. Sci. 9 (2008) 2146–2158.
[3] C.J. Mirocha, S.V. Pathe, B. Schauerhamer, C.M. Christensen, Appl. Environ. Microbiol. 32(1976) 553–556.
[4] C.J. Mirocha, in: W. Shimoda (Ed.), Conference on Mycotoxins in Animal Feeds and Grains Related to Animal Health, U.S. Food and Drug Administration, Rockville, MD, 1980, pp. 289–360.
[5] R. Wannemacher, S. Wiener, Medical Aspects of Chemical and Biological Warfare, vol. TMM8, U.S. Government Printing Office, Washington, DC, 1997, [Chapter 34].
[6] J.F. Grove, P.H. Mortimer, Biochem. Pharmacol. 18 (1969) 1473–1478.
[7] M.D. Grove, H.R. Burmeister, S.L. Taylor, D. Weisleder, R.D. Platner, J. Agric. Food Chem. 32 (1984) 541–544.
[8] C. Hansch, A. Leo, Exploring QSAR, American Chemical Society, Washington, DC, 1995.
[9] V. Betina, Chem. Biol. Interact. 71 (1989) 105–146.
[10] W.E. Steinmetz, P. Robustelli, E. Edens, D. Heineman, J. Nat. Prod. 71 (2008) 589–594.
[11] R.D. Cramer III, D.E. Patterson, J.D. Bunce, J. Am. Chem. Soc. 110 (1988) 5959–5967.
[12] G. Klebe, U. Abraham, T. Mietzner, J. Med. Chem. 37 (1994) 4130–4146.
[13] G. Klebe, U. Abraham, J. Comput. Aided Mol. Des. 13 (1999) 1–10.
[14] D. Young, T. Martin, R. Venkatapathy, P. Harten, QSAR Comb. Sci. 27 (2008) 1337–1345.
[15] B.B. Jarvis, G.P. Stahly, G. Pavanasasivam, J. Med. Chem. 23 (1980) 1054–1058.
[16] B.B. Jarvis, J.O. Midiwo, E.P. Mazzola, J. Med. Chem. 27 (1984) 239–244.
[17] M.S. Madhyastha, R.R. Marquandt, D. Abramson, Toxicon 32 (1994) 1147–1152.
[18] W.E. Steinmetz, B.L. Shapiro, J.L. Roberts, J. Med. Chem. 45 (2002) 4899–4902.
[19] L. Eriksson, J. Jaworska, A.P. Worth, M.T.D. Cronin, R.M. McDowell, P. Gramatica, Environ. Health Perspect. 111 (2003) 1361–1375.
[20] C.M. Wei, C.S. McLaughlin, Biochem. Biophys. Res. Commun. 57 (1974) 838–844.
[21] A. Jimenez, D. Vazquez, Eur. J. Biochem. 54 (1975) 483–492.
[22] D. Schindler, Nature 249 (1974) 38–41.
[23] M. Li, J.J. Pestka, Toxicol. Sci. 105 (2008) 67–78.
[24] J.L. Hansen, P.B. Moore, T.A. Steitz, J. Mol. Biol. 330 (2003) 1061–1075.